J. Fluid Mech. (1985), *vol.* 156, *pp.* 321–347
Printed in Great Britain

An experimental test of the theory of waves in fluid-filled deformable tubes

By J. H. GERRARD
Department of Aeronautical Engineering, University of Manchester

(Received 20 July 1984)

It seems that no treatment of pulsating flow in deformable tubes is complete without a reference to the work of Womersley (1955) which for an infinitely long tube deals with the waves of axisymmetric transverse motion and of longitudinal motion of the walls. This theory has so far been subjected to experimental test only for tethered tubes in which longitudinal wall motion is absent.

A series of measurements of the longitudinal motion has been made on horizontal water-filled latex tubes suspended by an array of strings so that there is minimal longitudinal constraint except at the ends, which are fixed. One end of the tube is driven by oscillating flow produced by a piston; the other end is closed. Theory and experiment agree when the tube is long provided an entrance length greater than a wavelength is included. Tubes which are short enough for reflection from the closed end to be significant present a more complicated problem. It is found that in the entrance length the theory of Womersley cannot be applied. A more refined theory is required which takes into account a distributed end constraint more completely than as a simple boundary condition.

Experiments on tethered tubes in which longitudinal wall motion is absent are also presented. These serve to demonstrate that the theory for such tubes agrees with measurements without any appreciable end effect and also shows that the small viscoelasticity of the latex rubber is correctly included.

1. Introduction

Womersley's (1955) theory of the waves accompanying pulsatile flow in deformable tubes is a much quoted reference in the literature of blood flow in arteries. It has been cited 55 times in the last 15 years at a rate which has not been diminishing. Womersley's theory concerns the wall motions in thin-walled infinitely long elastic tubes filled with incompressible fluid. The theory shows that there are two waves; a pulse wave in which the wall motions are principally radial and a second wave in which the wall motion is principally longitudinal. We shall call these waves I and II respectively. Womersley predicts the propagation constants γ_{I} and γ_{II} of these two waves in the practical case in which the wavelength is long compared with the tube diameter. In an elastic tube the propagation constants are functions of the non-dimensional frequency only. This non-dimensional frequency, which Womersley called α, is also known as the Stokes number and is equal to $R(n/\nu)^{\frac{1}{2}}$ where R is the internal radius of the tube, n the angular frequency and ν the kinematic viscosity of the fluid in the tube.

Womersley's theory and its results are to be found in all the recent texts on blood flow and related subjects; we may cite McDonald (1974), Talbot & Gessner (1973), Noordergraaf (1978) and Pedley (1980). In view of the simplicity of the measurements

which we shall describe it is surprising that the Womersley theory has not been experimentally investigated in its full form during the quarter century since it was published. There have been many theoretical treatments of the subject of waves in deformable tubes. These have considered refinements of the theory by the inclusion of factors such as thick walls, non-isotropic wall materials and viscoelastic effects, but without any essential change in the basic results. Cox (1969) compares various linear theoretical models. Rubinow & Keller (1978) extended the theory beyond the long-wavelength assumption of Womersley.

This paper addresses the basic physical problem of the wave motions in a latex rubber tube driven by an oscillating flow produced by a piston and the application of Womersley's theory to these. There are obvious applications to the theory of blood flow in arteries which will be referred to; the treatment of Womersley was written with medical applications in view. There are however great differences between arteries and latex tubes, such as the dependence of the elastic moduli on the applied stresses and their much greater viscoelasticity.

In the late 1960's there was concern that the longitudinal motion of arteries was much less than that predicted by Womersley. Atabek & Lew (1966) included the effects of initial stresses in the theory. There are large initial stresses in arteries but in the experiments that we shall describe they are small and their effect almost negligible. Mirsky (1967) showed that the longitudinal motion was reduced when the wall was elastically orthotropic (when $E_{\text{long.}} = \frac{1}{3}E_{\text{circ.}}$ where $E_{\text{long.}}$ and $E_{\text{circ.}}$ are the elastic moduli in the longitudinal and circumferential directions, the amplitude of longitudinal motion of the tube was reduced by 30 % in the aorta). In our experiments isotropic latex rubber tubes were used. Atabek (1968) showed that his analytical results for a thin-walled tube were only 3 % different from Mirsky's thick-wall analysis for the case where thickness/radius was 0.15; for our tube this ratio is 0.58 and account is taken of this by a correction factor.

Interest in this aspect of the subject waned, presumably because it was considered that in medical applications the relevant wave is the pulse wave in a tube which is tethered so that longitudinal motion is inhibited. In 1977 however van Loon, Klip & Bradley showed that, for arteries at *in-vivo* tension and length, the length and longitudinal force do not change when the pressure in the tube fluctuates. Large tethering forces are thus not necessary for the absence of longitudinal oscillations. This was found to be the case for large and small vessels and they suggested that this behaviour is a result of the structure of the vessels. Kuiken has recently (1984) shown that when the prestresses are included correctly in the wall equations the absence of longitudinal motion in arteries can be attributed directly to the large prestresses rather than to the tethering. Kuiken's publication also contains an analysis of a semi-infinite tube and the results which he presents indicate an end effect which extends over a large number of radii of the tube. This work could be eminently applicable to the present results. Calculations on the basis of this theory have not been applied to our configuration but further comment is made in §5.4.

Our interest in the subject arose from the observation that in a short section of a long rubber tube, which was unsupported except at the ends and not under tension, one could see the radial motion of the tube (of amplitude, say, 5 % of the diameter) whilst longitudinal motion was invisible. Womersley's theory predicts that the amplitude of the longitudinal motion should be considerably greater than that of the radial motion. Measurements of longitudinal and circumferential strains showed that the former was only about 1 % of the latter for a particular short segment whereas Womersley's theory predicts about 50 % at high α. The simple conclusion was that

tethering at points, at the ends of the segment, which are separated by very much less than a wavelength of the pulse wave effectively tethers the tube completely. The reason for this is that for nearly all of the time the whole segment is trying to expand or contract as a whole.

Measurements have been made on water-filled latex rubber tubes which were chosen because of their small viscoelasticity. The viscoelastic damping strongly affects the wave propagation and it is necessary even for latex to measure and include the viscoelasticity. That this is done correctly is tested by consideration of propagation in tethered tubes with no longitudinal motion. The latex tubes are shown to be elastically isotropic and it is assumed that the viscoelasticity is isotropic also.

Womersley's theory has not been tested experimentally partly because the theory concerns a tube of infinite length which is somewhat unrealistic. The tube has to have ends which produce a longitudinal (and radial) constraint. Away from the ends the constraints can be minimized and so a direct test of Womersley's theory is possible. We shall see that close to the end of the tube Womersley's theory must be replaced by one which includes the dominant end constraint but that far from the ends the direct application of Womersley's theory agrees with the measured values of longitudinal motion.

2. Womersley's theory

Since this paper concerns an experimental investigation of the results of Womersley's theory it is appropriate to outline his derivation (1955) and to include relations from the theory which we will need later but which are not given explicitly in Womersley's paper. His notation is adopted with the exception of the symbols used for the wall and fluid densities. The propagation constant is introduced as well as Womersley's complex wave speed.

The variables of the tube and the motion are shown in figure 1. The thin-walled elastic tube of density ρ_w is filled with incompressible fluid of density ρ. The fluid is subjected to a pressure gradient $\partial p/\partial z$. Womersley considers an infinite tube in which wave solutions are sought which have the form

$$q = q_1 \exp\left(in\left(t-\frac{z}{c}\right)\right) = q_1 \exp(int-\gamma z), \tag{1}$$

where $q = p$, u, w, ξ or ζ, which are defined on figure 1, n is the angular frequency, t the time and c the complex wave speed.

$$\gamma = \frac{in}{c} = \gamma_r + i\gamma_i = \gamma_r + \frac{in}{v}, \tag{2}$$

where γ_r and γ_i are the real and imaginary parts of γ and v is the real wave speed. Assuming p to be a given real quantity the other q_1's are complex because they have a phase different from that of p. Womersley's solutions are in terms of quantities which he calls c, c_0 and x, where

$$c_0 \text{ is the Moens–Korteweg speed} = \left(\frac{Eh}{2\rho R}\right)^{\frac{1}{2}}, \tag{3}$$

where E is Young's modulus. Table 1 gives expressions in terms of x, the quantity which Womersley chooses to use,

$$x = \frac{2}{1-\sigma^2}\frac{c_0^2}{c^2} = \frac{-2}{1-\sigma^2}\frac{\gamma^2 c_0^2}{n^2}, \tag{4}$$

where σ is Poisson's ratio.

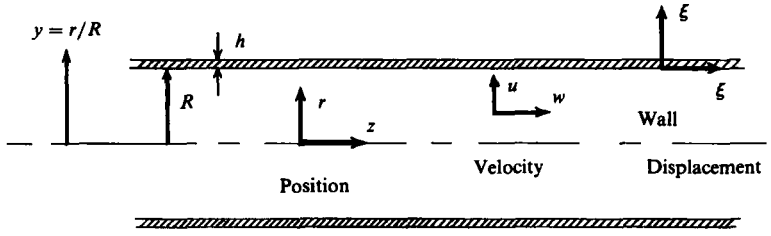

FIGURE 1. The variables of the tube and motion.

	In Womersley's variables	For Poisson's ratio = 0.5	In terms of γ	
$C_1/(p_1/\rho c^2) = \eta =$	$\dfrac{2\sigma-1+2/x}{F_{10}-2\sigma}$	$= \dfrac{-2}{x(1-F_{10})}$	$= \dfrac{3n^2}{4\gamma^2 c_0^2(1-F_{10})}$	(7)
$\dfrac{\xi_1}{R} =$	$\dfrac{p_1}{\rho c^2}\dfrac{\sigma(F_{10}-1+F_{10}/\sigma x)}{F_{10}-2\sigma}$	$= \dfrac{p_1}{2\rho c^2}\left\{1-\dfrac{2F_{10}}{x(1-F_{10})}\right\}$	$= \dfrac{-p_1\gamma^2(1+\eta F_{10})}{2\rho n^2}$	(8)
$\dfrac{n\zeta_1}{c} =$	$\dfrac{p_1}{\rho c^2}\dfrac{\mathrm{i}(1-F_{10}-2/x)}{F_{10}-2\sigma}$	$\zeta_1 = \dfrac{-\mathrm{i}p_1(1+\eta)}{\rho n c}$	$= \dfrac{-\gamma p_1(1+\eta)}{\rho n^2}$	(9)
$\bar{w}_1 =$	$\dfrac{p_1}{\rho c}(1+\eta F_{10})$		$= \dfrac{-\mathrm{i}\gamma p_1(1+\eta F_{10})}{\rho n}$	(10)

For a tethered tube ($\zeta = 0$)

$$\eta = -1, \quad p_1 = \frac{2\rho c_0^2}{1-\sigma^2}\xi_1/R$$

$\bar{w}_1$ is the amplitude of the cross-sectional mean speed of the fluid; ρ is the fluid density which Womersley calls ρ_0.

$F_{10} = 2J_1(z)/(zJ_0(z))$ where $z = \alpha \mathrm{i}^{\frac{3}{2}}$, J_1 and J_0 are Bessel functions of the first kind of order 1 and 0.

TABLE 1. Expression for variables in terms of pressure amplitude p_1

The linearized equations of fluid motion are reduced to expressions for w_1 and u_1 in terms of p_1 and a constant C_1 which is later eliminated. The radial and longitudinal equations of motion of the thin wall are

$$k\frac{\partial^2\xi}{\partial t^2} = \frac{p}{\rho R} - 2c_0^2\frac{\xi/R^2+\sigma\,\partial\zeta/\partial z/R}{1-\sigma^2}, \tag{5}$$

and

$$k\frac{\partial^2\zeta}{\partial t^2} = -\left(\frac{\partial w}{\partial y}+R\frac{\partial u}{\partial z}\right)_{y=1}\frac{\nu}{R}+2c_0^2\frac{\partial^2\zeta/\partial z^2+\sigma\,\partial\xi/\partial z/R}{1-\sigma^2}, \tag{6}$$

where $k = \rho_w h/\rho R$.

Matching the fluid and wall equations at $y = 1$ gives four equations in C_1/p_1, ξ_1/p_1, ζ_1/p_1 and c (or x or γ). The simpler case of zero longitudinal motion of the wall is simply obtained at this stage by inserting $\zeta_1 = 0$ in these equations; this case was formulated and discussed by Witzig (1914). Solution of the equations results in the expressions given in table 1 together with values for the wave speed and attenuation corresponding to two different values of the propagation constant or complex wave speed (and one value when $\zeta_1 = 0$). The wave speed is given by (2). The transmission factor per wavelength TF is defined as the factor by which the amplitude is multiplied to give the amplitude after transmission over a distance of one wavelength, λ.

$$TF = \exp(-\gamma_r\lambda) = \exp\left(\frac{-2\pi\gamma_r}{\gamma_i}\right). \tag{11}$$

For the tube with no longitudinal motion

$$\frac{c_0^2}{c^2} = \frac{1-\sigma^2}{1-F_{10}}, \tag{12}$$

$$\gamma^2 = \frac{-n^2(1-\sigma^2)}{(1-F_{10})\,c_0^2}. \tag{13}$$

The solution for the dependent variables are of the form

$$\zeta = \zeta_{\mathrm{I}_\pm} \exp(int \pm \gamma_{\mathrm{I}} z) + \zeta_{\mathrm{II}_\pm} \exp(int \pm \gamma_{\mathrm{II}} z), \tag{14}$$

representing one wave of each type travelling in each direction.

The value of the displacement ratio and strain ratio can be determined from Womersley's theory; these are

$$\frac{\xi}{\zeta} = 0.5R\gamma\left(\frac{1-F_{10}\eta}{1+\eta}\right), \tag{15}$$

$$\frac{\xi/R}{\partial\zeta/\partial z} = 0.5\left(\frac{1-F_{10}\eta}{1+\eta}\right). \tag{16}$$

For a tube with the internal radius used in the present work ξ/ζ is of the order of 0.01 for waves I and 0.0001 for waves II. The strain ratio is a function of α only and is of order 2 for waves I and 0.1 for waves II. In waves I the wall motion is principally radial and in waves II principally longitudinal. These waves are given a variety of names, Pedley (1980) calls them respectively the pressure wave and the shear wave. The pressure wave is similar to the one which is present in a tethered tube and in arterial systems and so might also be called the pulse wave; Kuiken (1984) and others call it the Young wave. The shear wave is so called because in wave transmission in elastic solids this describes the motion, which for this wave type has zero dilatation (these are also called secondary waves, equivoluminal waves and waves of distortion). In the present application the wave is not simply in the solid but in the liquid-filled tube as a whole; in this case they are often called Lamb waves. In Womersley's original treatment waves II were ignored which was reasonable considering the physiological application of the work. We shall proceed by considering waves in tethered tubes in which waves of only one type are present.

2.1. *Inclusion of wall thickness effect*

Womersley's theory is based on a membrane treatment of the wall. Taylor & Gerrard (1977) have shown that the wall thickness effect may be expressed as a multiplying factor, the thickness factor, θ_0, on the square of the inviscid wave speed so that c_0^2 becomes $c_0^2\theta_0$. They show that observations of the deformation of a thick-walled tube are represented to within 5 % at deformations (relative change of tube radius) of 20 % and more accurately for smaller deformations (hence the suffix 0 on θ). The expression for θ_0 is

$$\theta_0 = \frac{1+h/2R}{(1+h/R)^2}, \tag{17}$$

where h and R are the wall thickness and internal radius at zero excess pressure. The same thickness factor is obtained by different means in the thick-wall treatment of Whirlow & Rouleau (1965). It will be seen in §3 that the measured propagation constant for a tethered tube is in agreement with the thin-wall theory corrected by the inclusion of this thickness factor.

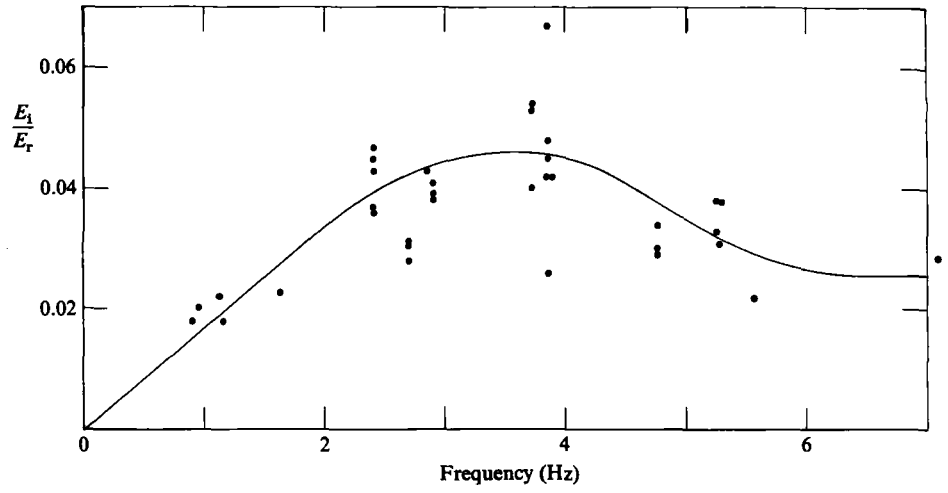

FIGURE 2. Viscoelastic characteristics of latex tube. Complex Young's modulus $E = E_r + iE_i$.

2.2. *The inclusion of wall viscoelasticity*

It is usual to represent the viscoelasticity of the wall by a Voigt model. The equation which describes oscillations in such a solid is that of an elastic substance with damping proportional to velocity. For a mass M oscillating on the end of a Voigt solid of length L and area of cross section A

$$M\ddot{x} + c\dot{x} + \frac{EA}{L}x = 0, \tag{18}$$

where E is Young's modulus. If the damping coefficient is zero but E is replaced by a complex value $E_r + iE_i$ the equation becomes

$$M\ddot{x} + \frac{E_i A}{nL}\dot{x} + \frac{E_r A}{L}x = 0. \tag{19}$$

Reference to Nolle (1950) shows that expressing the elastic modulus as a complex number is the usual practice in physiological applications. It is found that for artery walls the real and imaginary parts of Young's modulus are effectively constant above 2 Hz and below this frequency the imaginary part drops to zero at zero frequency (see Pedley 1980 p. 20). This implies that the material does not strictly conform to the Voigt model but since the viscoelasticity is small the approximations applied are adequate.

In the present experiments latex rubber tubes were chosen because of their small viscoelasticity. The viscoelastic characteristics of latex were determined by measurement of the logarithmic decrement of oscillations of weights suspended on various lengths of the experimental tube over the frequency range 0.85–7.1 Hz. The frequency and decay of amplitude were measured by suspending the rubber tube with a weight on the end from a flecture to which strain gauges were attached. The logarithmic decrement divided by π is the ratio E_i/E_r, the values of which are shown in figure 2. The scatter of the results was partly due to the motion of the tube not being purely longitudinal. Klip, van Loon & Klip (1967) found that E_i/E_r was 'frequency dependent and close to 0.02'. The difference between Klip's value and those of figure 2 will be shown not to have much effect in the application to a tethered tube but to be significant in the case of an unconstrained tube. The curve in figure 2

is drawn by eye in order to produce the dashed curve in figure 4(*a*) but it is also used in the calculations for the unconstrained tube. In view of this it is regrettable that the accuracy of E_i/E_r could not be improved but this is thought not to affect significantly the conclusions drawn.

3. Pulse propagation in a tethered tube

The investigation of waves in a tethered elastic tube serves to show that the application of Womersley's theory to this simple case agrees with experiment but more importantly that the effect of the viscoelasticity of the walls is properly included. We shall present some results of our own and also present the results of Klip (1962) and Klip *et al.* (1967) in a form different from that originally published but which shows more clearly the comparison with Womersley's theory. These two publications appear to be the most reliable and well documented. They cover a wide range of frequency and different tube diameters and wall thicknesses. They also used latex tubes as we have done. When other materials such as red rubber are used the study turns into one of the viscoelastic effects because these are so large, as in the work of Taylor (1959–60). There have also been comparisons of *in-vivo* data with Womersley's theory but this type of measurement is of little value for the testing of a physical theory which directly relates to a simple physical arrangement and not to the complicated natural phenomenon. The added difficulty of *in-vivo* measurements also reduces the accuracy of the comparison. These are of course important in the study of pulse propagation in mammalian arteries and do show the effect of viscoelasticity of the arterial walls; this is illustrated by the work of Milnor & Bertram (1978).

3.1. *Experimental method*

The apparatus used by Klip and Klip *et al.* was essentially the same as that used in the present work and will be briefly described after the current apparatus. A piston was driven in simple harmonic motion in a cylinder which connected to a metal tube of the same internal diameter as the latex tube. The latex tube was fastened over the end of this tube. The metal tube was fitted with a side branch with an attenuating constriction of small bore so that the oscillating flow propagated almost entirely down the latex tube. When measurements were made with a latex tube open at the far end a mean flow was supplied through the side branch.

Measurements were made of the oscillating pressures at various distances from the piston by means of Gould Statham P23Gb pressure gauges equipped with hypodermic needles which were inserted through the tube wall. It is essential that all air bubbles are removed from the cavity of the transducer. The cavity was connected through a valve to a syringe filled with boiled water with which the cavity could be flushed out. The waveforms from each gauge were simultaneously recorded on a digital transient recorder (Nicolet Instrument Corp. 1070 series). The data was transferred to magnetic tape for subsequent Fourier analysis by computer.

The latex tube was the only type available in the United Kingdom and was of 6.2 mm internal diameter with a wall thickness of 1.8 mm. These tube dimensions were measured from segments taken from each end of the experimental section. The wall thickness varied in a random fashion by 10% from sample to sample and over lengths of the tube of the order of a diameter. Calculations of the effect of this diameter variation showed that this caused the wave attenuation to increase by less than 5%.

The open-tube measurements were made with 4–5 m of straight tube followed by a 180° bend in the latex tube and a further length of 30 m of tubing. At the frequencies investigated the amplitude of the wave reflected from the end back to the straight section of the tube was attenuated to 3 % of the primary wave. Reflections from the bend were negligible.

The static Young's modulus E was measured by hanging weights on the latex tube. The modulus was also determined from strips cut longitudinally and circumferentially from adjacent parts of the tube; the values of E differed by only about 1 % thus demonstrating the isotropic nature of the latex. The values of the inviscid wave speed were determined from $c_0\sqrt{\theta_0} = (Eh/\rho D)^{\frac{1}{2}}$, (3). These values differed by as much as 8 %, from 14.36–15.50 m/s, over the period of the work and with different samples of latex. The higher value agrees with the E value used by Klip, the lower value appears to produce better agreement with experiments in §5. The variation of E is thought to be due to water absorption by the latex which certainly changes colour after extended use. The results in this section are presented non-dimensionally in such a way that they are independent of Young's modulus.

Measurements with a latex tube closed at the end remote from the piston were more accurate and could be performed with shorter lengths of tube. In this case there was no mean flow and the side tube was closed by a valve when the oscillating pressure measurements were made. Pressures were measured at six positions spaced along a tube of length 4.3 m. These included measurements at the closed end and at 20 mm from the piston end of the tube. The pressures at the latter position showed no signs of an entrance effect.

The latex tube was effectively tethered by lying it on the bench in the case of small amplitudes of oscillation as used in these experiments.

Klip's method of measurement was essentially the same as that employed here with the open tube. The piston and cylinder arrangement was different but had the same effect. The straight section of the tube was 4 m in length followed by 56 m or more of tube coiled in a helix. In all of the experiments the reflections from the end were small. The pressure amplitude at the end was always less than 5 % of that at the piston. The range of frequency was 0.33–33 Hz. The viscosity of the glycerol–water mixtures used was 1, 10 and 100 cP (1 cP = 10^{-3} Pa s). The tube diameters/wall thicknesses ratios were 12.36/0.84, 7.46/1.77 and 4.74/2.39 mm/mm. In this way a comprehensive range of parameters was covered.

In Klip's method and in some of our measurements the wave speed and attenuation were measured directly from the phase difference and amplitude ratio between two measuring stations a known distance apart in the straight section of the tube. A more accurate method which effectively averages several measurements is to determine by iteration the wave speed and attenuation which fits the measurements of phase and amplitude of the pressure at several points in a closed straight tube. The amplitude of the pressure in a tube extending from $z = 0$ at the piston to $z = L$ at the closed end is given by

$$p = \frac{p_0 \cosh(\gamma(L-z))}{\cosh(\gamma L)},$$

where p_0 is the pressure at $z = 0$ and γ is the propagation constant, the real and imaginary parts of which are adjusted by trial and error until a fit with the observations is obtained.

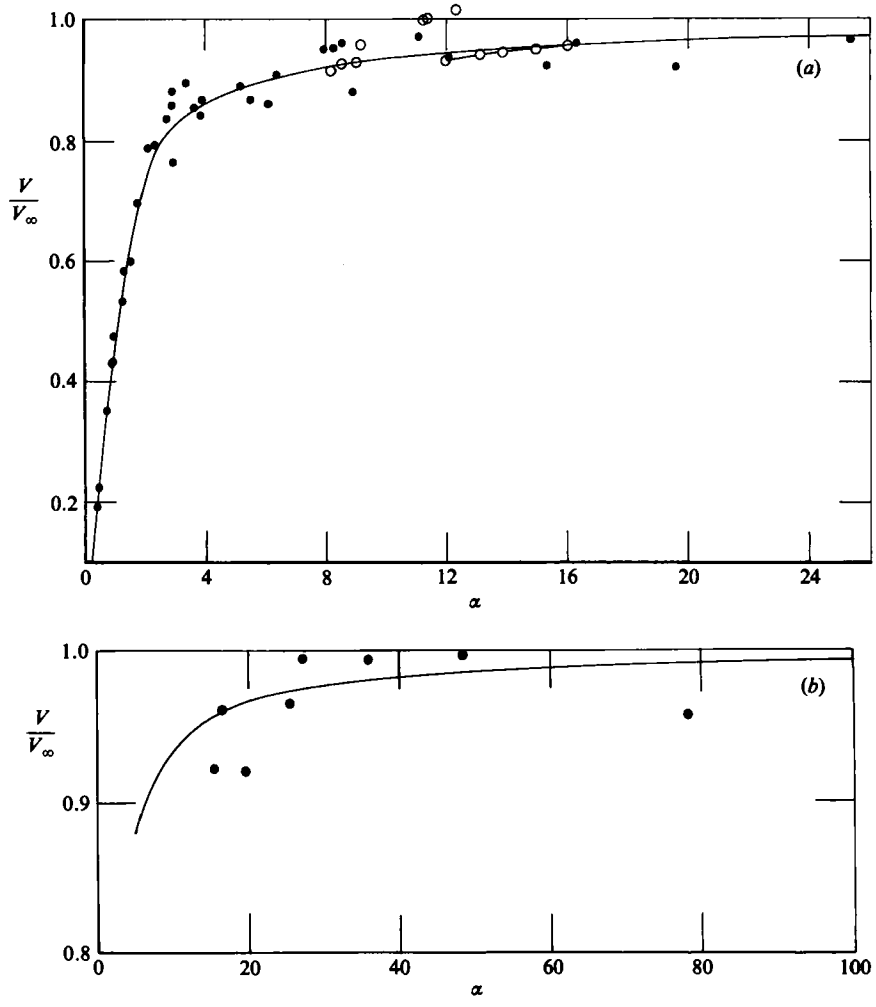

FIGURE 3. The ratio of tethered-tube wave speed to the inviscid wave speed ($\alpha = \infty$) as a function of Stokes number, α. The values of E_1/E_r in the range 0–0.04 make very little difference to the wave speed. ●, Klip *et al.* (1962, 1967). Present results: ○, pairs of points in open tube; ○—○, closed tube by adjustment of γ.

3.2. *Results*

The wave speed and transmission factor are shown in figures 3 and 4. The open circles joined by a curve are obtained from the present measurements in a closed tube. The other open circles are the present results obtained from single pairs of pressure measurements in a long open tube. The purpose here is to demonstrate that the values of the physical parameters of the latex are properly included and for this the results of Klip and Klip *et al.* are indispensible since they cover a wide range of all the parameters. The presentation of the Klip results has involved taking values from their graphs which has undoubtedly produced some scatter. The difference between this presentation and the original one is that the value of α is based on the mean radius of the tube which is calculated from the pressure–radius relation for a tethered tube given in table 1 and the thickness factor is included in the inviscid wave speed determined from the mean tube dimensions and the fluid kinematic viscosity. Though used in the calculation, the results presented are independent of this inviscid wave

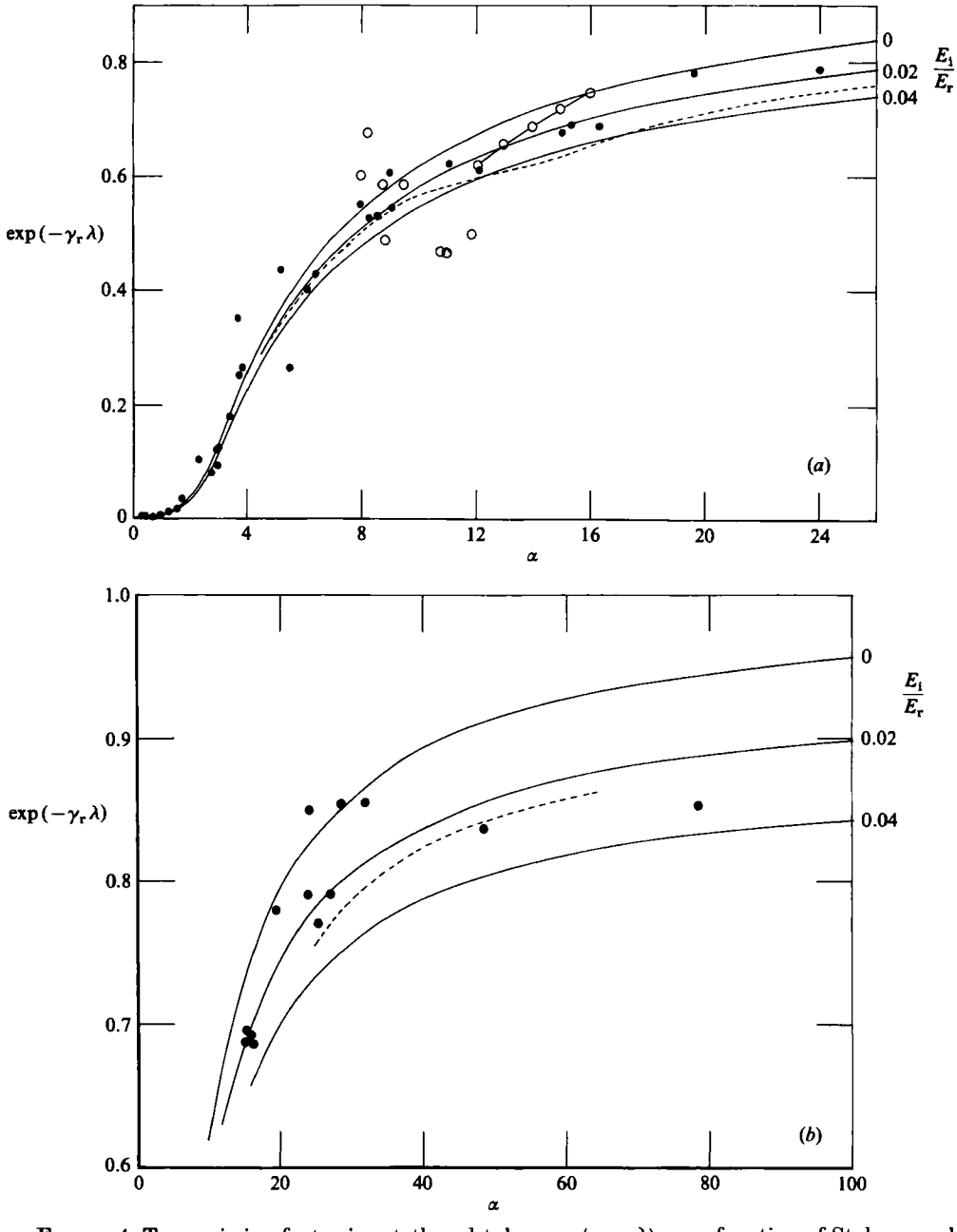

FIGURE 4. Transmission factor in a tethered tube, $\exp(-\gamma_r \lambda)$, as a function of Stokes number with E_i/E_r as a parameter. ---, E_i/E_r as in figure 2. Symbols as in figure 3.

speed. Klip's results are shown by ● symbols in figures 3 and 4. Also shown in the figures are the theoretical values for the ratios $E_i/E_r = 0$, 0.02 and 0.04. The wave speed is almost insensitive to changes in E_i/E_r and so only one curve is drawn. The transmission factor is sensitive to the value of this ratio and it is clear that the value 0.02 fits the data very well. The frequencies of the waves used in producing these figures from Klip's results covered the range 0.33–26 Hz. Figure 4 also shows the

dashed curve which corresponds to the E_i/E_r values of the curve in figure 2. The effect of this variation is only notable in the range of α from 10–20 where the differences from the constant E_i/E_r values is only small. Only one tube size was used in the present results and α variations reflect frequency changes. Klip's measurements with three tube sizes and fluid viscosity values give results in which high- and low-frequency determinations occur in the same range of α. There is no systematic variation between the scatter of the points and the frequency.

The results presented non-dimensionally in figures 3 and 4 are independent of the inviscid wave speed and hence of the elastic modulus of the tube material. This modulus is used to produce the non-dimensional values from Klip's values of wave speed and the real part of the propagation constant. Klip's values of these quantities show a difference between his calculated and measured values which appears and increases as frequency increases. The wave speed is proportional to the inviscid wave speed and the attenuation constant γ_r is inversely proportional. All the results in Klip's thesis (1962) show that at the higher frequency of 33 Hz the wave speed is 10% higher than the calculation and γ_r is some 15% lower. Some substances such as mammalian arteries have a dynamic Young's modulus up to twice the static value. It appears that for latex the elastic modulus is only increased by 10% at 33 Hz. In the measurements which will be presented for untethered tubes the highest frequency used was 4.5 Hz where we can expect the dynamic modulus to be only 1.4% higher than the static value.

The tethered tube results also show that any entrance and end effects are small (of the order of diameters rather than wavelengths). According to linear theory the oscillating velocity profile is the same in the rigid and in the tethered tube but there must be some entrance effect because the radial displacement is zero at the ends where the tube is clamped.

We conclude that the measurements in a tethered tube are in agreement with Womersley's theory. The accuracy of the comparison is determined principally by that of the determination of the Young's modulus of the tube material. The determination of the propagation constant of the waves in a tethered tube is a good method of determining the elastic modulus and its variation with frequency.

4. An untethered section of an otherwise tethered tube

In the course of the experiments on pulsatile flow in tethered latex tubes it was observed that small unsupported segments did not appear to possess any longitudinal motion even though the radial motion was apparent. At Stokes number greater than 5 Womersley's theory of the pulse wave (wave I) predicts that the longitudinal strain is about one half of the circumferential strain. For a longitudinal motion of ζ the strain is $\partial\zeta/\partial z$ and so the displacement ζ should be clearly visible. We now recognise that this is essentially the dilemma which in the 1960's prompted the interest in the calculation of the longitudinal motion.

Experiments were made to determine the relation of the longitudinal strain to the radial or circumferential strain. Measurements were made at the centre of a 165 mm segment of unsupported water-filled latex tube; the remainder of the tube was tethered. The apparatus and arrangement were exactly as in the experiments on long tethered tubes open at the end and with a mean flow as described in the last section. Adjacent to the measurement segment the tube passed through grooves in polyurethane foam blocks which prevented longitudinal motion. Under no tension the water filled tube was stiff enough to remain almost straight. The pressure

amplitude was small enough not to cause the tube to execute lateral oscillations (such a snaking motion predominates at high amplitudes if the tube is curved and not tethered). The measurement section was about 1 m from the piston end of the long tube. Mercury strain gauges were attached to the tube surface longitudinally and circumferentially close to and on each side of the centre of the segment. The gauge lengths were equal to one outside circumference of the tube and were cemented at their ends to the tube surface. The gauges were calibrated statically and dynamically. The dynamic calibration agreed with the static one up to the maximum strain of 4 % for the range of frequencies covered in the measurements. The amplified signals from the strain gauges were recorded on the transient recorder and then Fourier analysed to determine their amplitudes and phases. Pressure at the centre of the segment was also measured and analysed.

The measurements confirmed the visual observation that the longitudinal strain ϵ_L was very small compared with the circumferential strain, ϵ_C. The results of 16 measurements showed that

$$\epsilon_L/\epsilon_C = (1.24 \pm 0.46)\,\%$$

for a range of α of 4–17 obtained by varying the frequency from 0.3–5.0 Hz. There was no systematic variation with frequency. 28 readings of pressure p and strain were taken. The strain ϵ_C lagged p by $2 \pm 0.3°$ and the phase difference between ϵ_L and p was $180 \pm 10°$. In Womersley's pulse wave the phase difference between ϵ_C and p has a maximum value of 4.7° at $\alpha = 4$ and is less than 1° at $\alpha = 17$. For reasons which will become apparent in the next section no attempt at a more refined comparison with theory will be made here.

In these experiments the ratio of the length of the free segment to the wavelength of the pulse wave lay between 0.004 and 0.06. For almost the whole of the period of the oscillation, therefore, the segment is under tension of the same sign at all points of its length. Since the segment is stiff enough not to flex transversely it cannot change in length. We conclude that a tube which is tethered at points which are only a small fraction of a wavelength apart is effectively completely tethered.

5. The deformable tube with minimum longitudinal constraint

Having completed the preliminaries we are now in a position to embark upon the test of Womersley's theory. The conditions of zero constraint cannot be met in practice. The aim, therefore, is to use the minimum constraint to the longitudinal and radial motions of the tube. In view of the conclusions from the measurement of the motion of a free section of an otherwise tethered tube it follows that the tube needs to be several wavelengths long to approach freedom from end constraints and so that extensions in one half wavelength can be accommodated by contractions in the adjacent half wavelengths. This is complicated by the fact that the wavelengths of waves I and II are different. Almost all of the measurements have been made with a horizontal tube. If the tube is fixed at the ends at the same horizontal level and left free to hang loosely in between, the motion resulting from pulsating flow is principally a vertical transverse oscillation with nodes and antinodes. The minimum constraint which keeps the tube straight and horizontal is achieved by suspending it by closely spaced flexible ties which allow horizontal motion. This will be described more fully in §5.2 where reference is made to figure 5. The measurements have been made only of the amplitude of the longitudinal motion of the tube.

5.1. *Application of Womersley's theory to a closed tube*

Womersley's theory applies to an infinite tube or in practice to a tube section far from the constraints of the ends. The full solutions for longitudinal displacement and pressure which applies when there are reflections from both ends of the tube can be written,

$$\zeta(z) = C_1 \exp(-\gamma_{\mathrm{I}} z) + C_2 \exp(\gamma_{\mathrm{I}} z) + C_3 \exp(-\gamma_{\mathrm{II}} z) + C_4 \exp(\gamma_{\mathrm{II}} z), \tag{20}$$

$$p(z) = P_1 \exp(-\gamma_{\mathrm{I}} z) + P_2 \exp(\gamma_{\mathrm{I}} z) + P_3 \exp(-\gamma_{\mathrm{II}} z) + P_4 \exp(\gamma_{\mathrm{II}} z), \tag{21}$$

in which the pressure $p = p(z)\exp(int)$ and similarly for ζ. When the available boundary conditions are applied to these two equations one obtains four equations from which to determine the eight unknown quantities P_i and C_i but a general relation between the P_i and C_i can be used. To apply this theory to practical cases where the ends are not infinitely far away we assume, at least initially, that the infinite tube relations can be applied, that is, that p and ζ are related according to the Womersley theory as in (9) (table 1). This relation $\gamma p = -\rho n^2 \zeta/(1+\eta)$ applies for the positively travelling wave. For negatively travelling waves γ is replaced by $-\gamma$. For the positively travelling waves $\zeta(z) = C_i \exp(-\gamma_j z)$ and the pressure $p(z) = P_i \exp(-\gamma_j z)$ and so

$$\gamma_j P_i = \frac{\rho n^2 C_i}{1+\eta_j}, \quad j = \mathrm{I} \quad \text{or} \quad \mathrm{II}, \ \mathrm{i} = 1\text{–}4, \tag{22}$$

and for the negatively travelling waves

$$-\gamma_j P_i = \frac{\rho n^2 C_i}{1+\eta_j}, \tag{23}$$

and we will write this

$$= Z_j C_i \tag{24}$$

The boundary conditions are that $\zeta = 0$ at each end, $z = 0$ and L. At these ends also the velocity is related to the pressure gradient. At the closed $z = L$ end this velocity is zero. At $z = 0$ the deformable tube is attached to a rigid tube in which the fluid oscillations with a mean velocity equal to the piston speed, V_{p}. In the rigid tube

$$\frac{\partial p}{\partial z} = \frac{-\mathrm{i}\rho n V_{\mathrm{p}}}{1-F_{10}} = -MV_{\mathrm{p}}, \quad \text{say.} \tag{25}$$

The four equations, resulting from the application of the boundary conditions, which are to be solved for the C_i values are thus: from $\zeta = 0$ at $z = 0$,

$$C_1 + C_2 + C_3 + C_4 = 0; \tag{26}$$

from $\zeta = 0$ at $z = L$,

$$C_1 \exp(-\gamma_{\mathrm{I}} L) + C_2 \exp(\gamma_{\mathrm{I}} L) + C_3 \exp(-\gamma_{\mathrm{II}} L) + C_4 \exp(\gamma_{\mathrm{II}} L) = 0; \tag{27}$$

from $\partial p/\partial z = 0$ at $z = L$,

$$C_1 Z_1 \exp(-\gamma_{\mathrm{I}} L) + C_2 Z_1 \exp(\gamma_{\mathrm{I}} L) + C_3 Z_2 \exp(-\gamma_{\mathrm{II}} L) + C_4 Z_2 \exp(\gamma_{\mathrm{II}} L) = 0; \tag{28}$$

and from $\partial p/\partial z = -MV_{\mathrm{p}}$ at $z = 0$,

$$C_1 Z_1 + C_2 Z_1 + C_3 Z_2 + C_4 Z_2 = MV_{\mathrm{p}}. \tag{29}$$

These equations are easily solved to give the C_i and thus,

$$\zeta(z) = M' V_p \left\{ \frac{\exp(-\gamma_I z)}{1-\exp(-2\gamma_I L)} - \frac{\exp(-2\gamma_I L)}{1-\exp(-2\gamma_I L)} \exp(\gamma_I z) \right.$$
$$\left. - \frac{\exp(-\gamma_{II} z)}{1-\exp(-2\gamma_{II} L)} + \frac{\exp(-2\gamma_{II} L)}{1-\exp(-2\gamma_{II} L)} \exp(\gamma_{II} z) \right\}, \quad (30)$$

where $M' = M/(Z_1 - Z_2)$.

It needs to be pointed out that to find ζ at a particular value of z($\zeta = \zeta(z) \exp(int)$) the waves at that point must be summed taking account of their phase; the complex ζ values of the individual waves are added together. The resultant amplitude is the modulus of the added components.

5.1.1. *Extended entrance length*

We have seen that for a tethered tube agreement is obtained between measurements and the restricted theory which applies to this case. It was also found that end effects were minimal, being of the order of diameters of the tube. In the present case we shall see that the end effect has the wavelength as the characteristic length and so very long tubes are needed to check the simple theory. This is to be expected because the flow may be analysed in terms of a one-dimensional treatment in which the diameter of the tube only enters through the frequency parameter α. In this case the wavelength is the only length in the problem. An analytical treatment which reproduces the entrance length found in these experiments is obviously necessary but has not yet been formulated. This and the work of Kuiken (1984) will be discussed in §5.4. At the present stage of this work a simple exponential end effect factor will be applied to the results in order to show the form of the entrance length required. When the tube is not very long the entrance length will not have expired before the end of the tube is reached. In this case the entrance length may be extended to the waves reflected from the end. In order to do this an alternative derivation of the equation for $\zeta(z)$ is useful.

Consider waves of propagation constant γ (which may be γ_I or γ_{II}) radiating from $z = 0$,

$$\zeta = \zeta_0 \exp(int - \gamma z). \quad (31)$$

This wave is reflected, with change of phase to satisfy the $\zeta = 0$ boundary condition, successively at $z = L$ and $z = 0$, to give as the sum of all the reflections

$$\zeta = \zeta_0 \exp(int)\{\exp(-\gamma z) - \exp(-\gamma(2L-z))$$
$$+ \exp(-\gamma(2L+z)) - \exp(-\gamma(4L-z))\ldots\}, \quad (32)$$
$$= \zeta_0 \exp(int)\{\exp(-\gamma z) - \exp(-\gamma(2L-z))\}\{1 + \exp(-2\gamma L)$$
$$+ \exp(-4\gamma L) + \ldots\}, \quad (33)$$
$$= \frac{\zeta_0 \exp(int)\{\exp(-\gamma z) - \exp(-\gamma(2L-z))\}}{1-\exp(-2\gamma L)}, \quad (34)$$

which is the same as for each of the two waves in (30).

When there is an entrance length δ, we extend the entrance length into the reflections and the series above becomes,

$$\zeta = \zeta_0 \exp(int)\left\{\exp(-\gamma z)\left[1 - \exp\left(\frac{-z}{\delta}\right)\right] - \exp(-\gamma(2L-z))\right.$$
$$\left. \times \left[1 - \exp\left(\frac{-(2L-z)}{\delta}\right)\right] + \ldots\right\}. \quad (35)$$

This can be written as the original series of (32) minus the same series with γ replaced by $\gamma+1/\delta$ so that, for example, C_1 becomes

$$M'V_p\left\{\frac{1}{1-\exp(-2\gamma_I L)}-\frac{\exp(-z/\delta)}{1-\exp(-2(\gamma_I+1/\delta)L)}\right\}\exp(-\gamma_I z), \tag{36}$$

in (20) and similarly for the other C_i.

In the results which will be presented in the next section all the theoretical results with the extended entrance effect included are represented by open triangles, △. In some cases it appears that an end effect at both ends is required. In these cases a simple factor of

$$\left[1-\exp\left(\frac{-z}{\delta}\right)\right]\left[1-\exp\left(\frac{-(L-z)}{\delta}\right)\right] \tag{37}$$

is applied to the theoretical result of (30). The result is the same as with an extended entrance length, except near to $z = L$, when the tube is long. This simpler end-effect factor gives the results which are represented by open circles, ○.

5.1.2. *The constraint of the suspending strings*

When the tube is suspended on strings of length s, longitudinal motion is constrained by a restoring force due to the lifting of the tube as the strings swing in a pendulum motion. The square of the natural angular frequency of this motion is g/s, g being the acceleration of gravity. This constraint is allowed for after the manner of Womersley (1957) by replacing k, the non-dimensional mass per unit length of the tube in (6) by $k(1-g/sn^2)$.

5.2. *Apparatus and method of measurement*

The isotropic latex tube has small and known viscoelastic properties, that is, its elastic modulus is known as is the small damping. The tubes used were of the same diameter and wall thickness as those used for the tethered tube experiments. The original ones were perforated by the insertion of hypodermic needles and though these could be sealed, more uniform new tubes were preferred. The longest length in which latex tube is available is a nominal 15 m. In some experiments two such tubes were glued end to end. The experimental arrangement is shown in figure 5. In most of the work the tube was suspended to lie in a horizontal straight line. The long lengths were accommodated by suspending the tube from the handrail of a gallery in the laboratory. The suspension loops were sewing cotton, 370 mm long and separated along the tube 100 mm apart. The tubes were stretched by 5–10% in order to keep them straight. The small effect of this deformation was included in the calculation of the mean diameter which was determined from the static pressure–radius relation of Taylor & Gerrard (1977). One end of the tube was connected to the tube E which served as an entrance length to allow development of the oscillating-velocity profile (the same profile in a rigid as in a tethered deformable tube). The cylinder C and the piston P were of the same diameter as the inside of the tube. The piston amplitude and frequency were continuously variable. An infra-red detector, which was interrupted by a process on the piston driving rod, served to trigger a counter-timer which measured and displayed the period at frequenct intervals. The tube M which was closed by a tap just above the cylinder during the measurements of longitudinal motion was used to determine the mean internal pressure before the motion started. From this pressure the mean diameter was calculated. The end of the tube remote from the piston was closed and fixed rigidly. The tubes were filled with deionized water

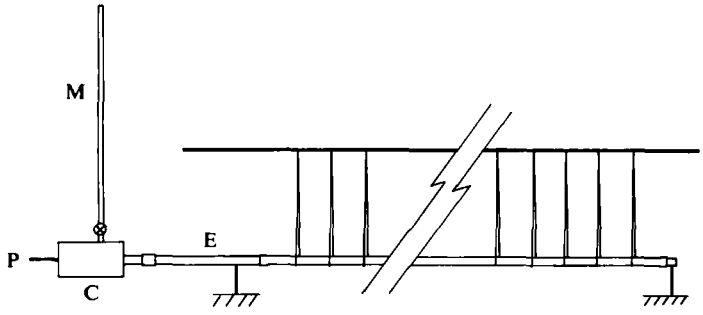

FIGURE 5. Experimental arrangement: M = manometer, P & C piston & cylinder, E = rigid entrance tube.

which was boiled to remove dissolved air. Care was taken to ensure that no bubbles remained in the tube. Measurements were made at a later stage to determine the effect of the bubbles. A bubble as large as two diameters in length located at either end of the tube was found to have no effect on the results.

The peak-to-peak longitudinal excursion of the tube wall was measured by viewing a line marked on the tube through a magnifying glass as it moved just below a transparent mm scale. The measurements of amplitude (half of the peak-to-peak excursion) were accurate and repeatable to 0.1 mm. Two sets of measurements were taken, either the amplitude at the centre of the tube was measured for a range of frequencies or the amplitude was determined as a function of distance along the tube for fixed values of the frequency. In one series of measurements tubes of length 4 and 5 m were suspended vertically by using a cranked entrance tube E and the amplitude at the centre of the length was observed. As before the tube was slightly stretched but there were no attachments to the tube except at the ends. In this condition the tube becomes tapered under the action of the hydrostatic pressure difference. A 5 m length of tube has a taper of included angle less than 0.01° which will have a negligible effect. These measurements were made in order to check that there were no unrecognized factors entering into the horizontal tube arrangement. The results, which are not presented here, showed that there were no such effects of any significance.

The tube lengths employed ranged from 4 to 34 m and the frequencies from 1 to 5 Hz. The tube inside diameter and wall thickness under zero excess pressure were 6.2 and 1.8 mm.

5.3. *Results*

Measured values of the amplitude of the longitudinal displacement in tubes of different lengths and over a range of frequencies will now be presented. Theoretical values are also shown on the same graphs. We start with cases which, sufficiently far from the ends, show agreement with the Womersley theory prediction. Figure 6 shows this with the longest tube, of length 34 m, and for the highest frequency used. This tube is sufficiently long to behave like a semi-infinite tube over most of its length. The experimental results are shown by solid square symbols, (the points determined lie at the centres of the symbols in this and the following figures). The undulating appearance is due to interference between waves I and II radiating from the entrance; reflection from the end has only a minor effect in this long tube. The amplitude of each of the waves I and II decays monotonically with distance down the tube owing to viscous attenuation and wall viscoelasticity once beyond the entrance length. The

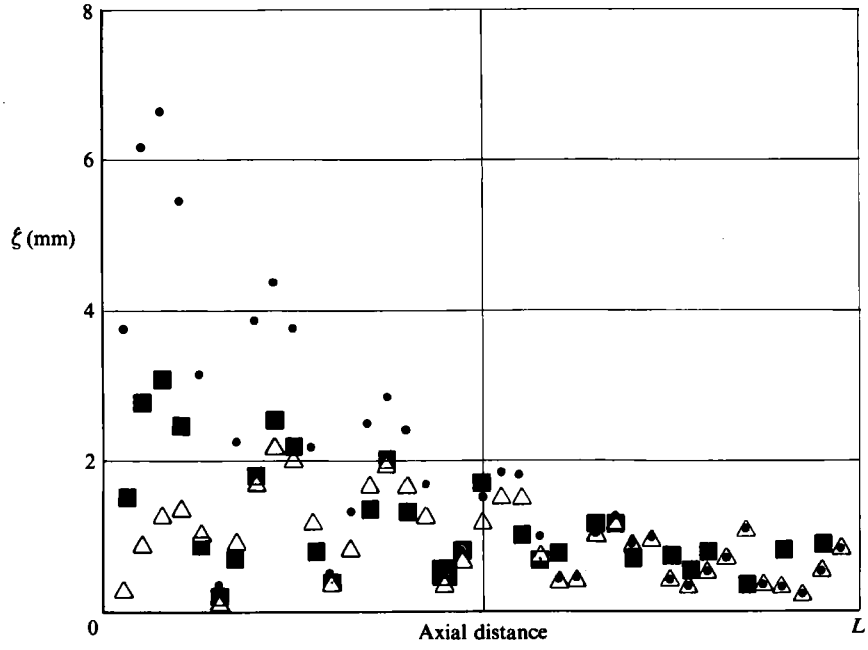

FIGURE 6. Axial motion amplitude ξ in tube of length L as a function of axial distance z. $L = 34.32$ m; $T = 0.22$ s; $\delta = 4.0\lambda_{\mathrm{I}}$; $\lambda_{\mathrm{I}}/L = 0.087$; $\lambda_{\mathrm{II}}/L = 0.202$: ■, experiments; ●, infinite-tube theory with displacement and velocity boundary condition at each end; △, extended entrance length, δ; ○, end effects at both ends, length δ_2.

value of E_1/E_r used to produce the theoretical values was taken from figure 2. At $T = 0.22$ s this value is 0.041. The value suggested by the work of Klip *et al.* (1967) is 0.02. If the latter value is used the theoretical values without any entrance length included have insufficient attenuation to come into agreement with the measurements in the second half of the tube. At the fourth and fifth maxima the present calculations have values of longitudinal amplitude of 1.85 and 1.28 mm; if $E_1/E_r = 0.02$ these values become 2.5 and 1.93 mm.

The principal wavelength of the undulations is the mean of the wavelengths of the two waves. The inviscid wavespeed used in the theory was that corresponding to the lowest Young's modulus measured and had the value $c_0\sqrt{\theta_0} = 14.36$ m/s. The wavelengths of the waves I and II were $\lambda_{\mathrm{I}} = 2.89$ m and $\lambda_{\mathrm{II}} = 6.93$ m. The direct application of Womersley's infinite-tube theory gives the values indicated on the figure. These points agree with the measured values beyond the entrance length with some unexplained discrepancy near to $z = L$. The entrance length will be quoted in terms of the wavelength λ_{I} which is proportional to the period T of the oscillations. Waves II have a longer wavelength which is proportional to T at small periods but at $T > 0.5$ s increases more rapidly with T. λ_{II} also depends on the mass per unit length of the tube, k in (6). In the tube used in the present experiments $\lambda_{\mathrm{I}} = 1.35T$, $\lambda_{\mathrm{II}} = 2.3\lambda_{\mathrm{I}}$ at $T < 0.5$ s, $\lambda_{\mathrm{II}} = 2.9\lambda_{\mathrm{I}}$ at $T = 0.9$ s. As well as values directly calculated from Womersley's infinite-tube theory the values obtained after an application of an entrance length are also shown. At the highest frequencies very large entrance lengths of $4\lambda_{\mathrm{I}}$ are required in order to produce agreement with measured values. The value $4\lambda_{\mathrm{I}}$ is critically dependent on the viscoelastic characteristic E_1/E_r. This entrance length produces much too large a reduction in the first wavelength up to $z = 0.15L$. There is no foundation for the assumption that in the entrance length the variation

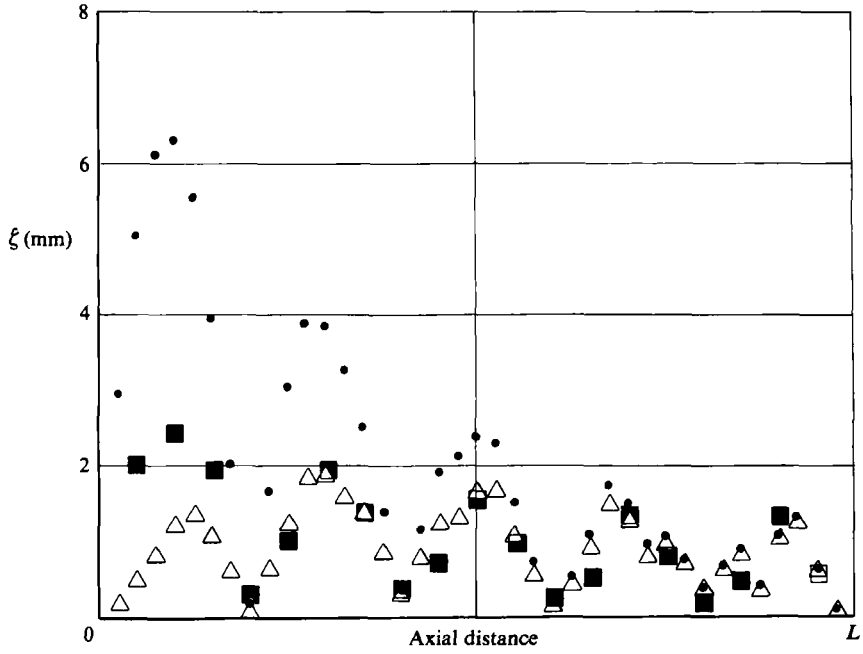

FIGURE 7. Axial motion amplitude $\hat{\xi}$ in tube of length L as a function of axial distance z. $L = 34.32$ m; $T = 0.29$ s; $\delta = 4.0\lambda_1$; $\lambda_I/L = 0.114$; $\lambda_{II}/L = 0.267$. Symbols as in figure 6.

should be of the simple exponential type. This correction is applied simply to show that an entrance effect of some sort is required. The mechanism of the entrance effect will be discussed later. The values of the entrance length are not accurately determined. The values quoted are the result of computation with trial values until reasonable fit with the experimental results was obtained.

Figure 7 at a lower frequency is similar to figure 6 but shows better agreement at large z. The theoretical results at large z possess small wavelength undulations not present in the measurements. As the wavelength-to-tube-length ratio λ_I/L increases in the following figures this appearance of undulations not present in the measured values becomes more pronounced. Figures 7 and 8 have the same value of λ_I/L and are very similar. In figure 9 in which the value of λ_I/L is almost twice the value in the previous figures we notice a peak in the theoretical amplitude at $z/L = 0.7$ where the measurements show a trough. It also seems as if an end effect is required to reduce the theoretical amplitude close to $z = L$. In figure 10 at $\lambda_I/L = 0.28$ the theory indicates four maxima whereas the experiments show only two. A similar situation is seen in figure 11 in which the inclusion of an end effect (at $z = L$) produces better agreement.

Figures 12–15 show results for the 15 m tube which was the shortest for which measurements of ζ as a function of z were made. It is clear from these results that the application of entrance and end effects in an effort to make theory and experiment agree is becoming meaningless. In these results λ_I/L is of the order of unity and a full theory of the end effect is necessary. The effect of changing the propagation constant of the waves II is shown on these figures. This is accomplished by altering the value of k in (6). This change in the tube mass per unit length by a factor of 0.25 has little effect on the wave I but the wave II value of γ_r is increased by 20% and γ_i decreased by 37%. This is inclined to show that in the entrance length in tubes

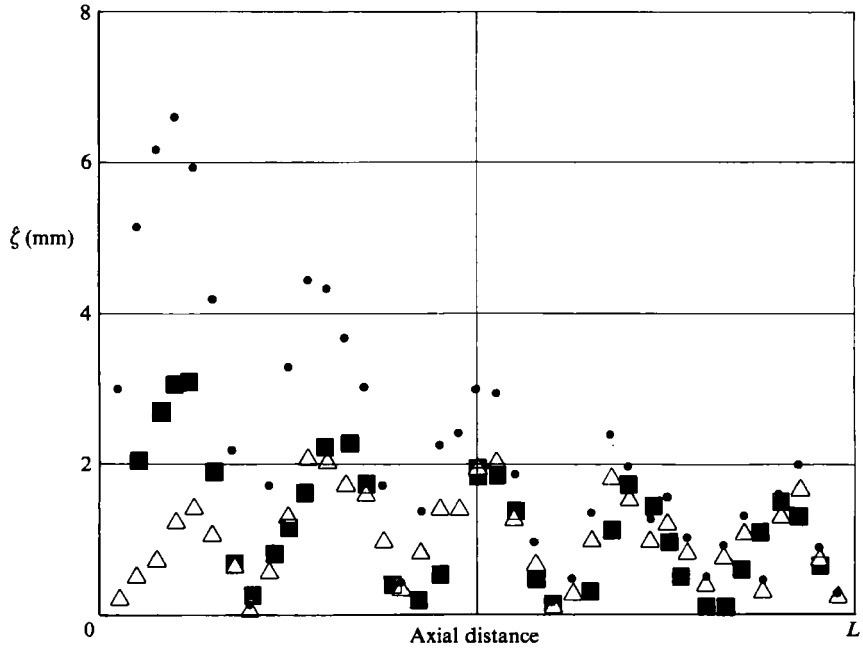

FIGURE 8. Axial motion amplitude ξ in tube of length L as a function of axial distance z. $L = 26.00$ m; $T = 0.22$ s; $\delta = 4.0\lambda_{\mathrm{I}}$; $\lambda_{\mathrm{I}}/L = 0.115$; $\lambda_{\mathrm{II}}/L = 0.267$. Symbols as in figure 6.

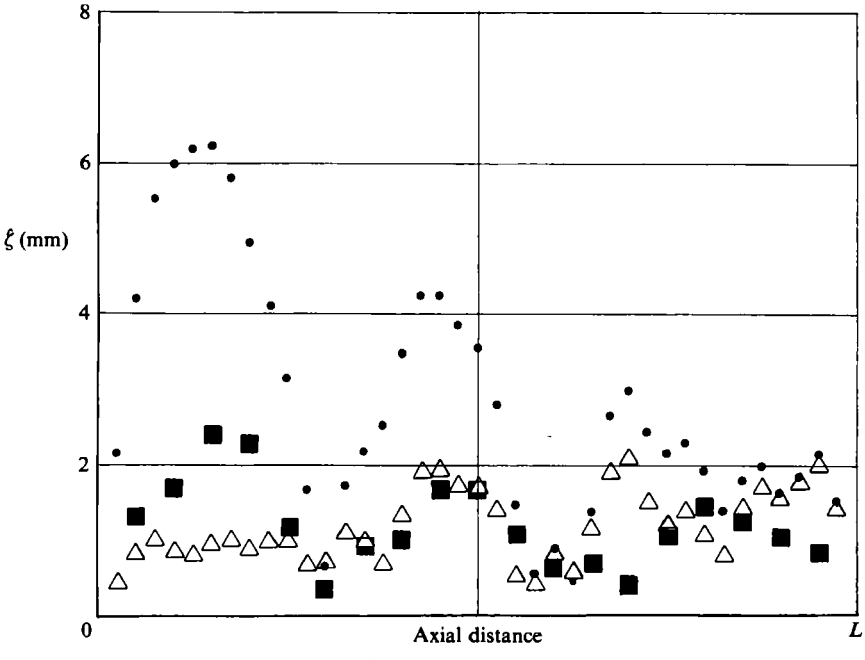

FIGURE 9. Axial motion amplitude ξ in tube of length L as a function of axial distance z. $L = 34.32$ m; $T = 0.45$ s; $\delta = 4.5\lambda_{\mathrm{I}}$; $\lambda_{\mathrm{I}}/L = 0.177$; $\lambda_{\mathrm{II}}/L = 0.422$. Symbols as in figure 6.

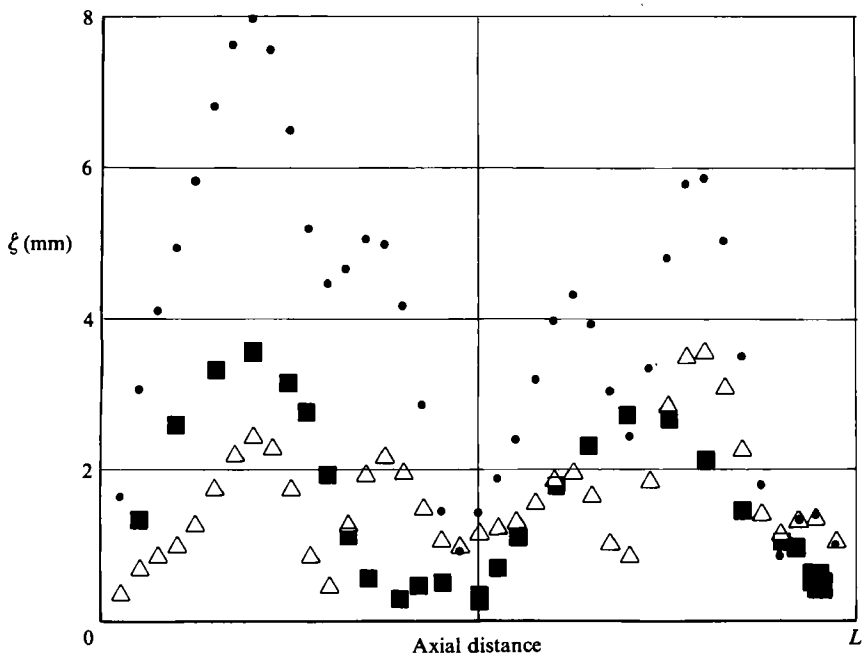

FIGURE 10. Axial motion amplitude ξ in tube of length L as a function of axial distance z. $L = 26.00$ m; $T = 0.55$ s; $\delta = 4.5\lambda_{\mathrm{I}}$; $\lambda_{\mathrm{I}}/L = 0.286$; $\lambda_{\mathrm{II}}/L = 0.696$. Symbols as in figure 6.

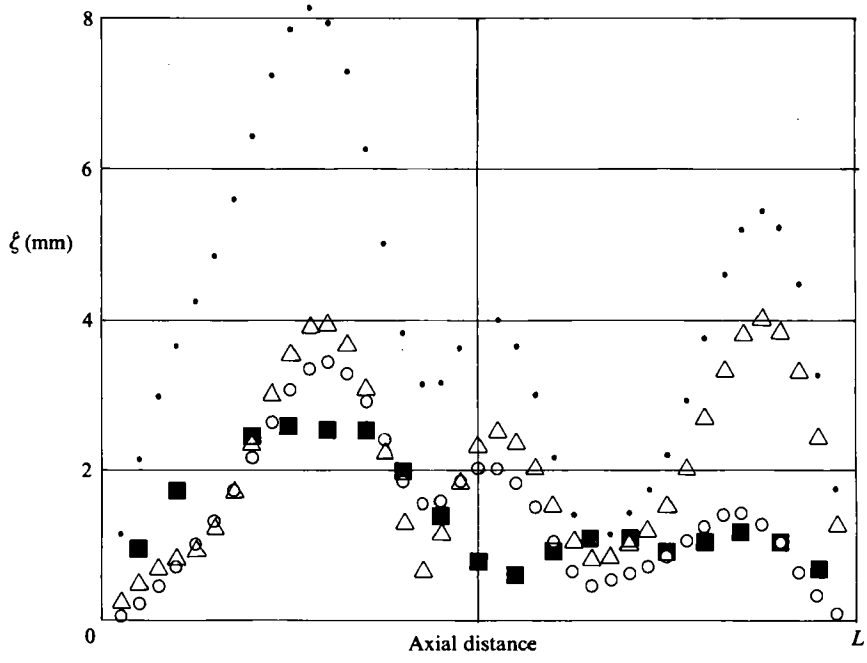

FIGURE 11. Axial motion amplitude ξ in tube of length L as a function of axial distance z. $L = 26.00$ m; $T = 0.775$ s; $\delta = 2\lambda_{\mathrm{I}}$; $\delta_2 = 1\lambda_{\mathrm{I}}$; $\lambda_{\mathrm{I}}/L = 0.403$; $\lambda_{\mathrm{II}}/L = 1.0732$. Symbols as in figure 6.

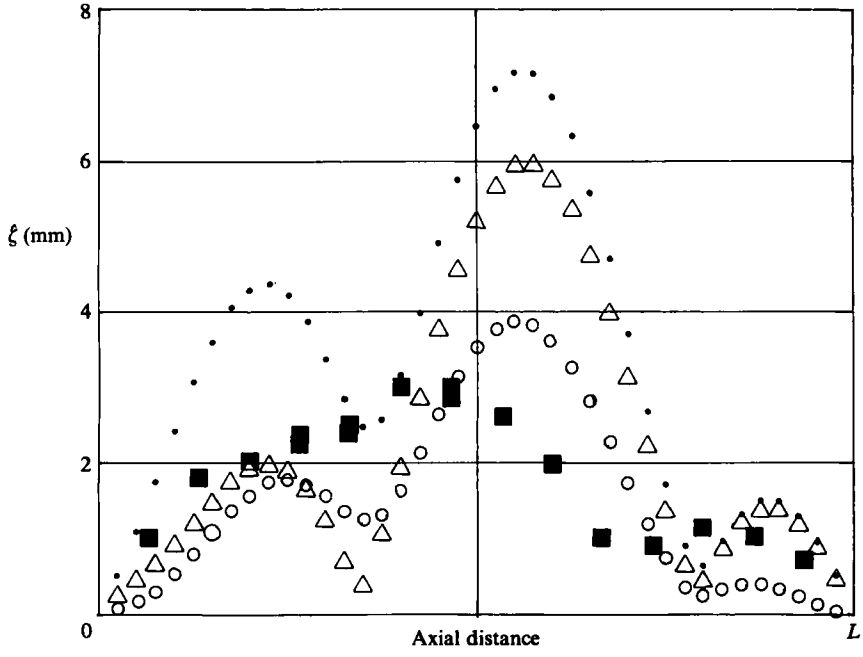

FIGURE 12. Axial motion amplitude ξ in tube of length L as a function of axial distance z. $L = 15.00$ m; $T = 0.665$ s; $\delta = 0.625\lambda_{\mathrm{I}}$; $\delta_2 = 0.625\lambda_{\mathrm{I}}$; $\lambda_{\mathrm{I}}/L = 0.599$; $\lambda_{\mathrm{II}}/L = 1.516$. Symbols as in figure 6.

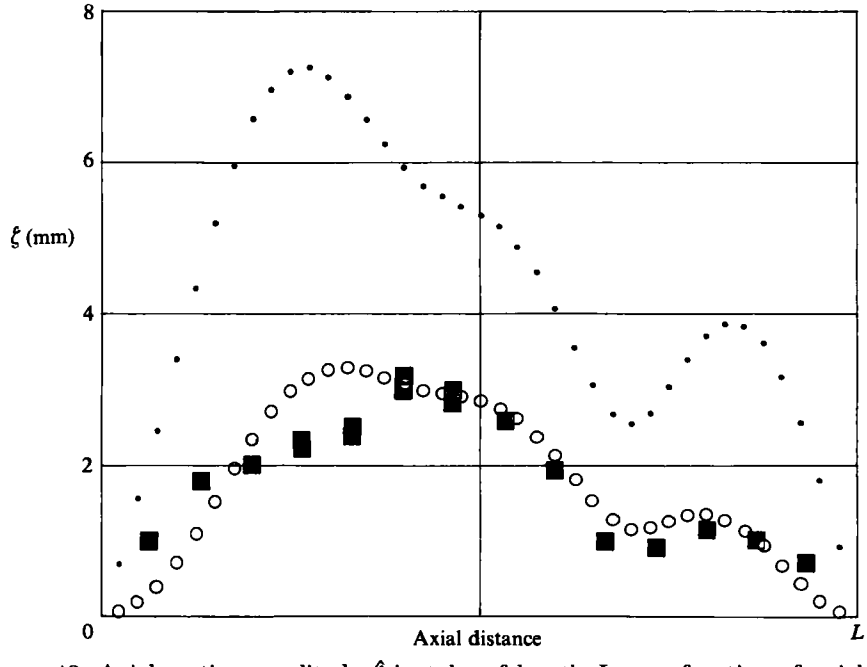

FIGURE 13. Axial motion amplitude ξ in tube of length L as a function of axial distance z. $L = 15.00$ m; $T = 0.665$ s; $\delta_2 = 0.625\lambda_{\mathrm{I}}$; $\lambda_{\mathrm{I}}/L = 0.600$; $\lambda_{\mathrm{II}}/L = 2.07$. Mass per unit length of the tube in the theory reduced to 0.25 times actual value, symbols as in figure 6.

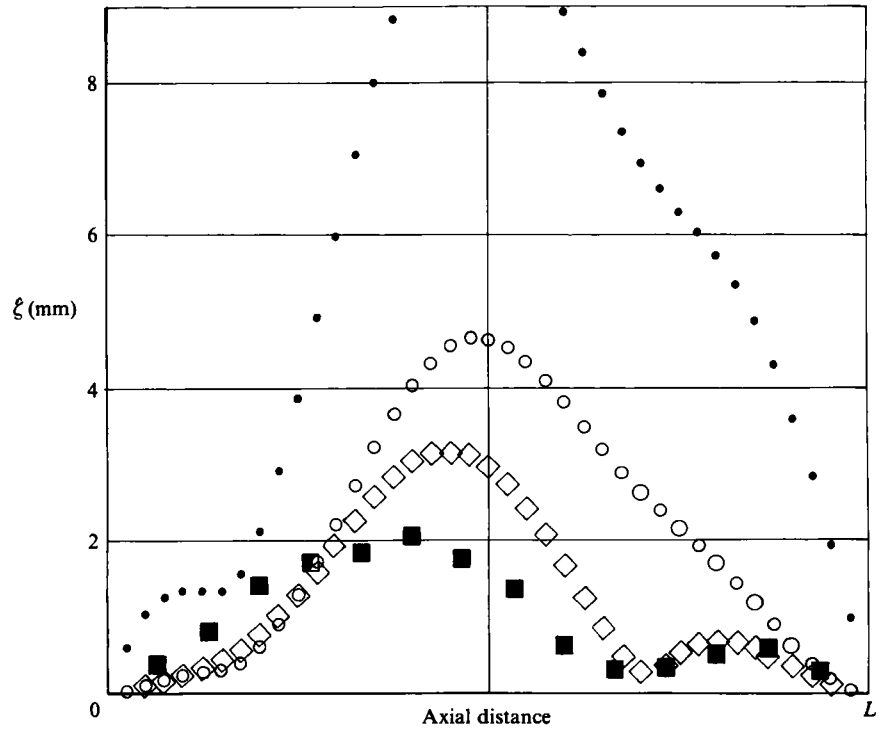

FIGURE 14. Axial motion amplitude ξ in tube of length L as a function of axial distance z. $L = 15.00$ m; $T = 0.80$ s; $\delta_2 = 0.625\lambda_I$; $\lambda_I/L = 0.723$; $\lambda_{II}/L = 1.958$. ◇, mass per unit length of the tube in the theory reduced to 0.25 times the actual value. Other symbols as in figure 6.

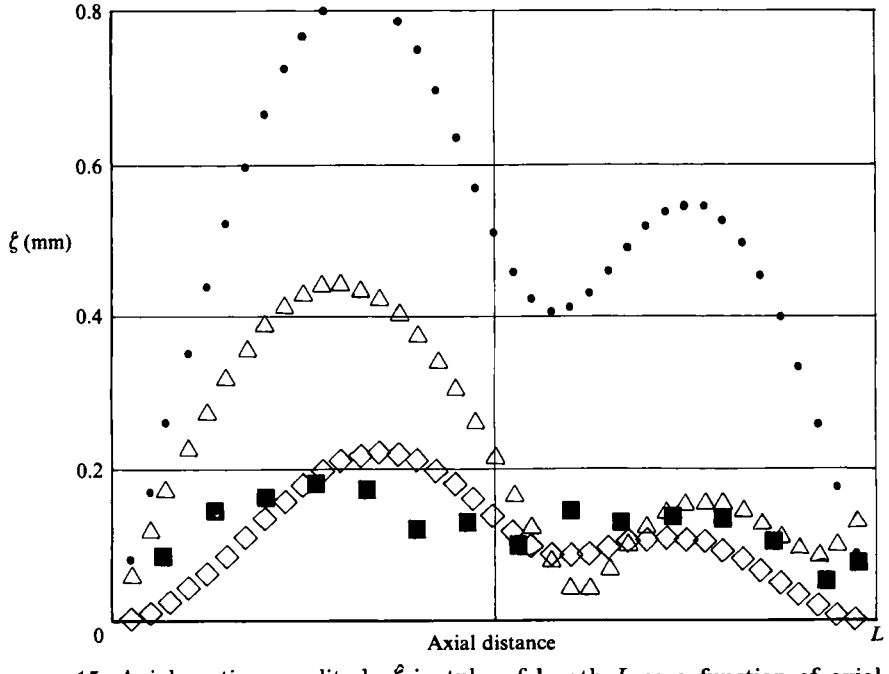

FIGURE 15. Axial motion amplitude ξ in tube of length L as a function of axial distance z. $L = 15.00$ m; $T = 1.01$ s; $\delta = 2.0\lambda_I$; $\lambda_I/L = 0.916$; $\lambda_{II}/L = 2.974$. ◇ as in figure 14, $\delta_2 = 0.625\lambda_I$. Other symbols as in figure 6.

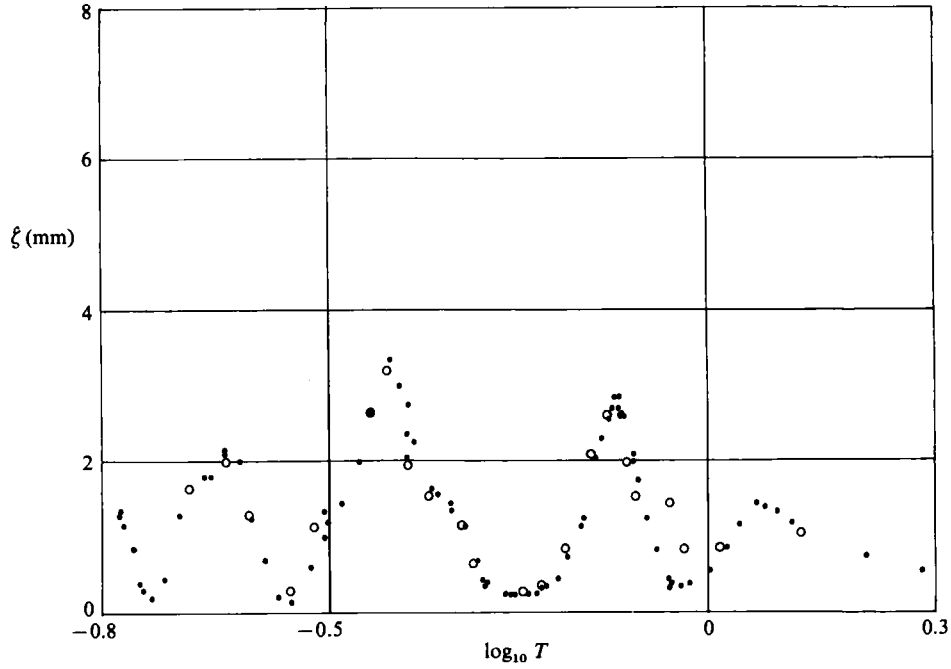

FIGURE 16. Axial motion amplitude $\hat{\zeta}$ at $z = \frac{1}{2}L$ as a function of the logarithm to the base 10 of the period, $L = 26.0$ m. ●, initial extension 10%; ○, initial extension 4%.

not long compared with the wavelength the departures from Womersley's theory are so large that a single correction factor cannot be considered and that a different full theoretical treatment must be embarked upon; there is an indication that the propagation constant changes in the entrance length.

The remaining results which will be presented show the variation of longitudinal motion amplitude at the centre of the tube, $z = \frac{1}{2}L$, as a function of the period of oscillation. Figure 16 shows the experimental results at the centre of the 26 m tube. In the whole range of periods in figure 16 the length of the tube in wavelengths varies from about 12 to $1\lambda_{\mathrm{I}}$ and about 5 to less than $0.5\lambda_{\mathrm{II}}$. The initial tension in the tube required to keep it straight was here varied between the limits employed in all the other experiments. This change is seen to produce no significant effect at most frequencies but there are large effects at a period just less than one second. This effect was not further investigated. It was noticed that at some frequencies some of the tubes executed sideways oscillation of maximum amplitude of 1 cm. This is to be expected when the tube length is close to an odd integral number of half wavelengths. In this situation the tendency for the whole tube to change its length is at a maximum. The longitudinal motion directly resulting from the sideways motion is negligibly small and so the effect of sideways motion was ignored. It appears that this needs further investigation. The initial extension of less than 10% is only included in the theory through the change in internal radius which is used to calculate α. This effect is very small. A curve drawn through the experimental points of figure 16 is reproduced with the theoretical values in figure 17. This figure clearly shows that Womersley's theory for the infinite tube, plus boundary conditions, agrees well with the measurements when the measurement position is remote from the end in terms of wavelengths. As the wavelength of the oscillations increases with increasing

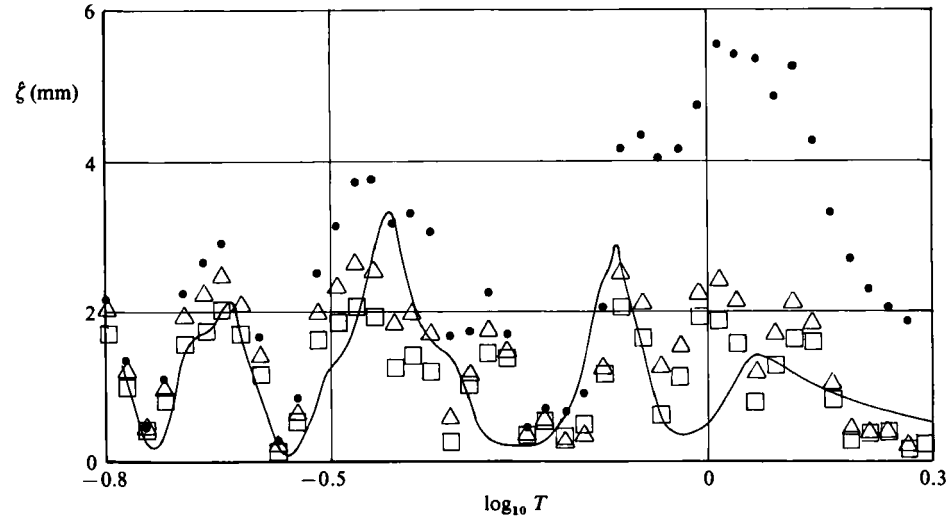

FIGURE 17. Experimental results of figure 16 ——, compared with theory: ●, infinite-tube theory with displacement and velocity boundary conditions at each end; △, $\delta = 2.5\lambda_1$; □, $\delta = 4.0\lambda_1$.

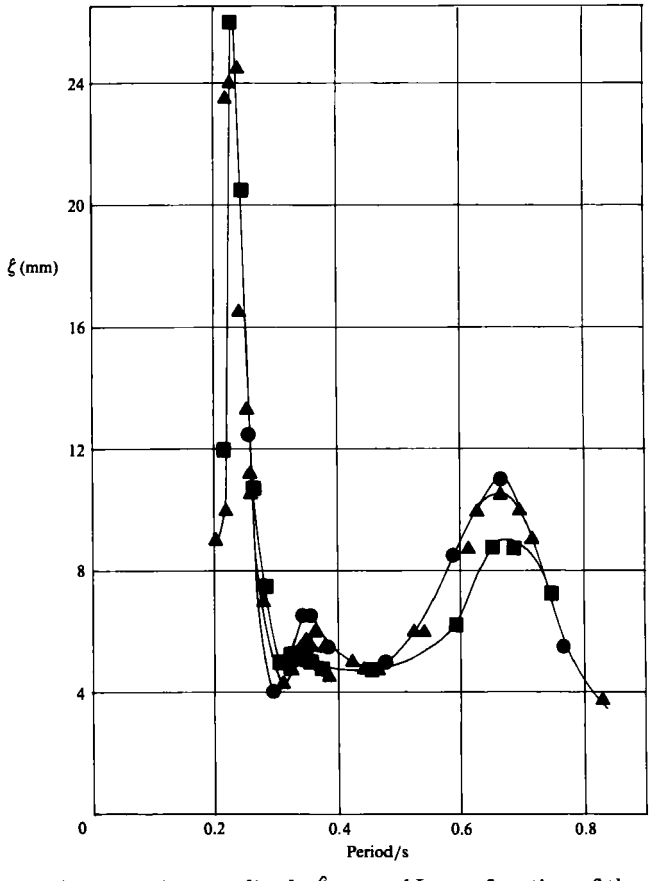

FIGURE 18. Axial motion amplitude ξ at $z = \frac{1}{2}L$ as a function of the period, $L = 5.03$ m: ●, ▲, ■, initial extensions = 1, 5 and 9 % respectively.

period the end effect encompasses the measurement position and ever increasing departures from the theory are encountered.

The effect of initial extension is shown in figure 18. Increased initial tension almost suppresses the peak at a period of 0.35 s. The theoretical results which are not shown also indicate three peaks at about the same values of the period. The maximum amplitudes calculated were 9, 14 and 18 mm in order of ascending period. Not surprisingly there is no agreement with measurement in this relatively short tube.

5.4. *Discussion*

To summarize the results of the experiments we may say that Womersley's theory agrees with experiment far from the constraint of the ends of the tube. There is some indication that there may be an end effect at the closed end remote from the piston. At the piston end of the tube there is an entrance effect which considerably reduces the amplitude calculated from the infinite-tube theory. The entrance length is several wavelengths in extent.

Womersley's relationships indicate the changes which take place as the waves propagate down the tube. At the entrance the piston produces a sinusoidally oscillating flow and pressure. This fluid pressure causes the tube to expand in accordance with (8) of table 1. This equation is complex which implies a phase difference between radial displacement and pressure and hence in one cycle of oscillation the energy transferred to the wall is not all recovered. The difference in energy is radiated into the wave of the other type. This is quite apart from any loss of energy due to viscoelastic effects. In the case of wave I which is the principal wave initially, the radial expansion has a concomitant longitudinal contraction (due to Poisson's ratio and in this case the incompressibility of latex). The attendant longitudinal stress sets up waves II which propagate (more slowly than waves I) away from the position of deformation. Similarly, because (8) applies to both types of wave, waves II produce waves I also. These mechanisms of energy transfer occur in an infinite tube and away from the ends in our case they are automatically included in the theory. The application of the end conditions ($\zeta = 0$) determines the amplitude relation between waves I and II but is applied at a position at which it appears that the infinite tube theory is not valid; the manner in which wave I produces wave II is different near to the ends of the tube. In order to solve the equations for the longitudinal displacement in a closed tube we assume the infinite-tube relation between pressure and this displacement. At the entrance the wave I starts as a wave in a tethered tube because the tube is fastened to the rigid extension of the piston cylinder; also the velocity profile in the rigid tube is the same as that in a tethered tube. The propagation constants are therefore expected to vary in the entrance length.

The simple exponential factor applied to the calculations to produce agreement with the measurements in tubes long compared with the wavelength has been presented to show that some entrance length is necessary. Two facets of this are worth comment. The wavelengths of the undulations in figures 6–9 are in agreement with the infinite-tube theory with constant propagation speeds. It is only in tubes which are of the order of one wavelength long that there is evidence for the need for the propagation constant to vary. The second point to make is that the simple entrance factor presented in the figures relating to long tubes does not produce good agreement in the first wavelength at the piston end of the tube. It is not clear whether this is an effect of being close to the entrance or an effect of the proximity of a fixed end. The values of the entrance length in wavelengths used to produce agreement with

measurement seem not to vary strongly with the period of oscillation. The shorter tubes used at the longer periods reflect the fact that the first cycle requires a lower entrance length in the longer tubes at smaller values of the period.

The recent work of Kuiken (1984) has two main contributions. He corrects previous work which includes initial stresses in the tube and shows that these are of paramount importance in arteries. In the present work the initial stresses are small; his non-dimensional prestresses, S' longitudinally and T' circumferentially, are in our case respectively less than 0.3 and 0.05. That the longitudinal tension produces a small effect has been seen in figures 16 and 18. More important for the present work is his treatment of the semi-infinite tube extending from $z = 0$–∞ and which changes from being free to move only radially at $z \leqslant 0$ to being unconstrained both radially and longitudinally at $z > 0$. Solutions are no longer simply proportional to $\exp(int - \gamma z)$. Kuiken's results for both waves I and II show a variation of wavespeed and transmission factor with z at α values between 10 and 60. The range of z covered is from 0–40 tube radii. The results certainly show an effect of the sort which we are seeking but there is no indication of the propagation constant approaching the infinite tube value at large z. The experimental results are presented as data to challenge the ingenuity of the theoreticians. Our current work involves a medical application of the numerical analysis of pulsatile flow in distensible tubes. It is intended to test the numerical method on the results presented here. This exercise could produce ideas which might aid further analytical work.

5.5. *Conclusions*

Experiments have been made on one size of latex rubber tube nominally 6.2 mm internal diameter and 1.8 mm wall thickness in various lengths. With the aid of the results of Klip *et al.* on tethered latex tubes it was shown that the viscoelastic characteristics which we measured agree with their results. The viscoelasticity affects the attenuation of waves in the tubes and vitally affects the test of Womersley's theory. It was found that this theory of wave motion in an unconstrained tube could only be directly tested very far from the ends of a tube driven by oscillating flow introduced at one end. To possess a region free from end constraints the tube needed to be several wavelengths long. The two propagation constants of Womersley's waves which we have called waves I and II have both to be correctly predicted to produce the wave amplitudes measured. Simple measurements of the amplitude of the longitudinal motion of the wall have served to test the theory.

It is found that Womersley's theory does predict the measured amplitude at distances beyond four wavelengths of wave I from the entrance to the tube. This implies that the simple boundary condition following from the tube being fixed in position and diameter at the ends adequately represents the end when it is viewed from a distance. Close to the end the infinite unconstrained tube the relationships of Womersley are insufficient to predict the amplitude which is measured to be less than half of the theoretical value. There is some evidence that there is an end effect at the closed end but the main effect observed is at the entrance. In this region a new analytical treatment is awaited or the application of Kuiken's (1984) analysis. It appears from the experimental results that at least one propagation constant is not in fact constant in the entrance region. This is arguable on physical grounds from the manner in which the wave II is produced.

The cooperation of Willem Klip who supplied a copy of his thesis and helpful comments is gratefully acknowledged. The experiments on tethered tubes were made

in the University of Manchester Department of Surgery. The valuable assistance and encouragement of David Charlesworth, Reader in Surgery was vital to the initial stages of this work.

REFERENCES

ATABEK, H. B. 1968 Wave propagation through a viscous fluid contained in a tethered, initially stressed, orthotropic elastic tube. *Biophys. J.* **8**, 626.

ATABEK, H. B. & LEW, H. S. 1966 Wave propagation through a viscous incompressible fluid contained in an initially stressed elastic tube. *Biophys. J.* **6**, 481.

COX, R. H. 1969 Comparison of linearized wave propagation models for arterial blood flow analysis. *J. Biomech.* **2**, 251.

KLIP, W. 1962 *Velocity and Damping of the Pulse Wave.* The Hague: M. Nijhoff.

KLIP, W., VAN LOON, P. & KLIP, D. A. 1967 Formulas for phase velocity and damping of longitudinal waves in thick-walled viscoelastic tubes. *J. Appl. Phys.* **38**, 3745.

KUIKEN, G. D. C. 1984 Wave propagation in a thin-walled liquid-filled initially stressed tube. *J. Fluid Mech.* **141**, 289.

MCDONALD, D. A. 1974 *Blood Flow in Arteries*, 2nd edn. Arnold.

MILNOR, W. R. & BERTRAM, C. D. 1978 The relation between arterial viscoelasticity and wave propagation in the canine femoral artery in vivo. *Circ. Res.* **43**, 870.

MIRSKY, I. 1967 Wave propagation in a viscous fluid contained in an orthotropic elastic tube. *Biophys. J.* **7**, 165.

NOLLE, A. W. 1950 Dynamic mechanical properties of rubberlike materials. *J. Polymer Sci.* **5**, 1.

NOORDERGRAAF, A. 1978 *Circulatory System Dynamics.* Academic.

PEDLEY, T. J. 1980 *The Fluid Mechanics of Large Blood Vessels.* Cambridge University Press.

RUBINOW, S. I. & KELLER, J. B. 1978 Wave propagation in a viscoelastic tube containing viscous fluid. *J. Fluid Mech.* **88**, 181.

TALBOT, S. A. & GESSNER, U. 1973 *Systems Physiology.* Wiley.

TAYLOR, M. G. 1959–60 An experimental determination of the propagation of fluid oscillations in a tube with a viscoelastic wall; together with an analysis of the characteristics required in an electrical analogue. *Phys. in Med. & Biol.* **4**, 63.

TAYLOR, L. A. & GERRARD, J. H. 1977 Pressure–radius relationships for elastic tubes and their application to arteries. *Med. & Biol. Eng. & Comput.* **15**, 11.

VAN LOON, P., KLIP, W. & BRADLEY, E. L. 1977 Length–force and pressure–volume relationships of arteries. *Biorheol.* **14**, 181.

WHIRLOW, D. K. & ROULEAU, W. T. 1965 Periodic flow of a viscous liquid in a thick-walled elastic tube. *Bull. Math. Biophys.* **27**, 355.

WITZIG, K. 1914 Uber erzwungene Wellenbeivergungen zaher, inkompressibler Flussigkeiten in elastischen Rohren. Inaug. Dissertation, University of Berne, Switzerland.

WOMERSLEY, J. R. 1955 Oscillatory motion of a viscous liquid in a thin-walled elastic tube I: The linear approximation for long waves. *Phil. Mag.* **46**, 199.

WOMERSLEY, J. R. 1957 Oscillatory flow in arteries: the constrained elastic tube as a model of arterial flow and pulse transmission. *Phys. in Med. & Biol.* **2**, 178.